Identification of Emergent and Floating Aquatic Vegetation Using an Unsupervised Thresholding Approach: A Case Study of the Dniester Delta in Ukraine

Ioannis Manakos[1], Eleftherios Katsikis[1], Sergiy Medinets[2], Yevgen Gazyetov[2], Leonidas Alagialoglou[1] and Volodymyr Medinets[2]
[1]*Information Technologies Institute, Centre for Research and Technology Hellas, Thessaloniki, Greece*
[2]*Odesa National I.I. Mechnikov University, Odesa, Ukraine*

Keywords: Wetland, Sentinel-2, Floating Vegetation, Emergent Vegetation, Thresholding, Multi-Class Segmentation.

Abstract: Monitoring of emergent and floating vegetation in freshwater ecosystems is of high importance for water management in an area. This study proposes a methodology for the automatic monitoring of aquatic vegetation using indicators estimated via remote sensing image analysis. The study area is located in the Lower Dniester Basin in Southern Ukraine. The approach is developed using Sentinel-2 images and validated with field measurements. The goal is to discriminate and map three classes of aquatic surface condition; namely, areas covered with floating vegetation, or dominated by emergent vegetation, and open water. The approach is transferable across different dates over a period of three years. Results are useful for governmental authorities and natural/ national park administrations for near real-time monitoring of aquatic vegetation to mitigate the impact of overgrowth on water quality, biodiversity, and ecosystem services.

1 INTRODUCTION

Freshwater ecosystems, being a valuable resource of ecosystem services for local population wellbeing and regional economy (*e.g.*, drinking water production, tourism, aquaculture, hydropower generation), are vulnerable to anthropogenic impacts (Sutton *et al.*, 2011). The core driver of ecological concerns in many transboundary river catchments, including the Dniester, is excessive nutrients load of anthropogenic origin as a result of agricultural, industrial (via wastewater discharges and re-deposition of gas emission), domestic (via sewage discharges) and other anthropogenic activities (*e.g.* Medinets *et al.*, 2016, Medinets *et al.*, 2020a, Medinets *et al.*, 2020b), which leads to a significant increase of eutrophication in the river-deltas, their lakes, and adjacent estuaries (Kovalova *et al.*, 2021).

Moreover, temperature increase and precipitation pattern alteration under changing climate, together with fluvial water flow disturbance due to up-regulation with hydro power constructions, often enforce and intensify negative impacts on biodiversity, biological resources, and ecosystem services (Rouholahnejad *et al.*, 2014). Along with algal blooms, all this is also subjected to the overgrowth of aquatic vegetation, which is often observed in vulnerable deltaic areas.

Aquatic plants (emergent, floating and submerged), being natural components of most water bodies and playing an important role in aquatic ecosystem functioning, when overgrown or bloomed, often lead to harmful consequences for water quality, biodiversity, ecosystem functioning and services provision via

- decreasing dissolved oxygen level,
- increasing pH,
- reducing light penetration, slowing water velocity (while increasing water temperature),
- increasing siltation rates (in slow streams),
- serving as mechanical substrates for filamentous algae,
- clogging or hampering navigation channels/ areas used for fishing and touristic purposes, and
- losing recreational/ touristic attractiveness (Greenfield *et al.*, 2007; Hussner *et al.*, 2017).

Therefore, the near real time (semi-) automatic monitoring of aquatic vegetation cover coupled with the identification of its different types/ species is of high value for authorities and natural/ national park administrations. However, they are still a big challenge in shallow water bodies.

Manakos, I., Katsikis, E., Medinets, S., Gazyetov, Y., Alagialoglou, L. and Medinets, V.
Identification of Emergent and Floating Aquatic Vegetation Using an Unsupervised Thresholding Approach: A Case Study of the Dniester Delta in Ukraine.
DOI: 10.5220/0012024000003473
In *Proceedings of the 9th International Conference on Geographical Information Systems Theory, Applications and Management (GISTAM 2023)*, pages 98-103
ISBN: 978-989-758-649-1; ISSN: 2184-500X

Various histogram-based methods for automatic earth observation features' estimation exist in the literature, which are based on satellite imagery (Kordelas *et al.*, 2018). Furthermore, based on the success of machine learning methods in other applications, (Chen *et al.,* 2018) utilized decision trees for mapping underwater vegetation, while the study of Espel *et al.* (2020) compared the Random Forest and the Support Vector Regression algorithms for estimating submerged macrophyte cover from very fine-scale resolution (50 cm) multispectral Pléiades satellite imagery, and showed that both algorithms have promising performance metrics. Further studies aimed at classifying floating vegetation in various water bodies using Sentinel-2 images. The results showed that the classification accuracy was dependent on the density (Midwood *et al.*, 2010; Valta-Hulkkonen *et al.*, 2004), and the species (Ade *et al.*, 2022) of the floating vegetation.

In this study, an approach is developed for automatic monitoring of aquatic vegetation, by discriminating and mapping three main classes usually met in freshwater ecosystems (floating, emergent vegetation, and open water-no vegetation). Several indicators, which are derived by algebraic combinations of the satellite bands, are exploited within a multicriteria hierarchical analysis approach on top of a verified unsupervised thresholding approach (Kordelas *et al.*, 2018, 2019; Manakos *et al.*, 2019). The proposed approach has been developed and validated within the WQeMS H2020 project (Grant Agreement No. 101004157) using reference and satellite data of the Dniester River, which were initially registered by the authors for the needs of ENI CBC BSB PONTOS project (Grant Agreement No. BSB 889).

2 MATERIALS AND METHODS

2.1 Study Area

The study area is located in the Lower Dniester Basin, covering the Dniester Delta and the adjacent Dniester Estuary (Southern Ukraine) with a total area of roughly 1800 km^2 (Fig. 1), including the Lower Dniester National Nature Park (LDNNP). The Dniester is the largest transboundary river in the Western Ukraine and Moldova, discharging to the Black Sea. The Lower Dniester Basin is located within the Black Sea lowland, consisting of steppe plains. The topography is a gently dipping plain, which contributed to the development of extensive wetland area in the floodplain of the river, dissected

Figure 1: Study area of the Dniester Delta (red boundaries) and the territory occupied by the Lower Dniester National Nature Park (dashed area), overlaid on a Google Earth image snapshot.

by branches, ancient riverbeds that are often flooded (OSCE, 2005).

The pilot area has a temperate continental climate. Annual mean air temperature is 10.5°C (period of 2000-2014) varying from 8.4°C to 12.5°C (Medinets *et al.*, 2016). The long-term average annual precipitation sum was 464 mm (2000-2014) but varied substantially over the last years from 420 mm (in 2020) to 771 mm (in 2021). The atmospheric total N (TN) deposition rate is moderate at *ca.* 11.4 kg N ha^{-1} y^{-1} (Medinets *et al.*, 2020b) with around 67% contribution from organic constituents. Such large contribution is also observed for open waters in the northwestern part of the Black Sea (Medinets and Medinets, 2012; Medinets, 2014).

2.2 Satellite Imagery

Sentinel-2 (Level 2A) products are downloaded from the Copernicus European Space Agency (ESA) hub for the dates 11/08/2018, 05/08/2020, 30/08/2020, 05/08/2021. The acquired products refer to the tile T35TQM.

2.3 Validation Data

Direct measurements of aquatic vegetation boundaries were performed by field GPS tracking using a boat in the north part of the Dniester Estuary by the Odesa National I.I. Mechnikov University (ONU) on an annual basis (in July) over 2010-2021

within the national projects studying Dniester ecosystems funded by the Ministry of Education and Science of Ukraine. This approach included the following stages:

- Tracking of the boundaries of emergent and floating vegetation with the boat-mounted GPS device of Eagle SeaCharter 640CDF GPS with horizontal accuracy of 3-5 m (when it was impossible to distinguish floating vs. dense semi-submerged vegetation, a sum of both was indicated as a floating vegetation).
- Visual assessment of emergent and floating vegetation, its types and covered areas with a photo report.
- Post-expeditionary processing of geolocation data was carried out. GPS data was downloaded and converted into a coordinate system suitable for the Geographical Information Systems (GIS) software.
- In a GIS software, the position of the aquatic vegetation boundaries was checked and manually corrected (where required) using available spaceborne images (LandSat 5, 7, 8 and Sentinel-2), since in some areas it was not possible to bypass the aquatic vegetation polygons on a boat (small vessel), because of dense vegetation cover or the presence of other difficulties.
- Spatial analysis of aquatic vegetation polygons was performed using a GIS software, which included the corrections for boat indentation from the vegetation boundaries, the production of digital maps of emergent and floating vegetation cover, and the analysis of spatiotemporal variations of emergent and floating aquatic vegetation in certain sectors of the Dniester Delta (Fig. 2). The studied area was divided into 5 sectors according to the geohydromorphological characteristics: (i) Sector A: a north part of Dniester estuary with extensive wetland area on the right bank of the river (76.3 km^2); (ii) Sector B: the territory between two branches (Deep Turunchuk and Dniester) of the Dniester river (81.2 km^2); (iii) Sector D: the territory of the Dniester branch mouth with adjacent area (20.3 km^2); (iv) Sector E: the territory of the left bank of the Dniester branch and the Karaholsky bay (26.9 km^2); (v) Sector F: an open water central part of the Dniester Estuary (51.6 km^2).

The ground reference data, which were used in this study, were collected on 22/07/2018, 05/08/2020 and 26/07/2021, and utilized for validation as follows:

- Ground data on 22/07/2018 were used to assess the validity of the predictions on 11/08/2018;
- Ground data on 05/08/2020 were used to assess the validity of the predictions on 05/08/2020 and 30/08/2020;
- Ground data on 26/07/2021 were used to assess the validity of the predictions on 05/08/2021.

Due to cloud conditions some dates of the ground and the satellite data acquisitions are zero (0) to twenty-five (25) days apart. The effect is considered negligible for the development of the plant communities during this period; however, the effect is visible in the results and discussed, accordingly.

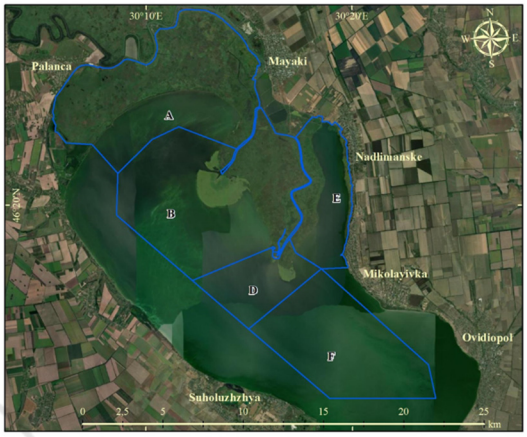

Figure 2: Location of sectors used for spatiotemporal analysis of the emergent and floating vegetation cover in the deltaic part of the Lower Dniester.

2.4 Methodology

An unsupervised approach was applied to map the study area in three aquatic vegetation classes: namely, i) open water, ii) emergent vegetation, and iii) floating vegetation. The workflow is broken down in three phases.

In the first phase the Sentinel-2 bands B04 (red), B08 (near infrared; NIR), and B11 (shortwave infrared; SWIR) are initially utilized to classify the area in the land, open water and emergent vegetation classes following the thresholding method suggested in Kordelas *et al.*, 2018 (Fig. 3).

All pixels with value smaller than the value of the first deep valley (left Fig. 3 – left arrow) are classified as open water. The emergent vegetation is identified in the area, where following conditions apply:

a) the pixel value of the SWIR's band histogram is between the value of the first and the second deep valley (Fig. 3 left – between left and right arrow), and
b) the pixel value of the Normalized Difference Vegetation Index (NDVI; (B08+B04)/(B08-B04)) histogram is after the first deep valley which is greater than the value 0.3 (Fig. 3 right – after the arrow).

The rest area is classified as land, and renamed to unclassified, as this category is not of direct interest for the aquatic vegetation mapping.

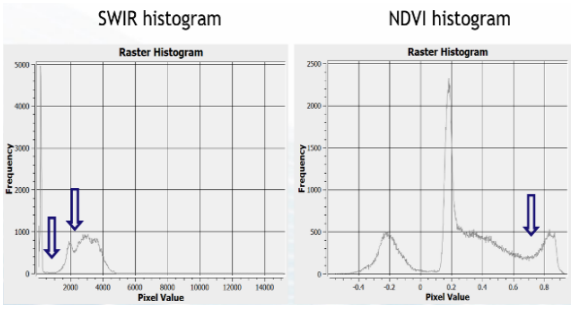

Figure 3: Open water (left Figure - left arrow) and emergent vegetation (left Figure – right arrow & right figure arrow) thresholds, estimated on the SWIR band (left Figure) and the NDVI (right Figure), respectively (image acquisition date: 30/08/2020).

In the second phase additionally Sentinel-2 bands B05 (red edge; RE) and B12 (shortwave infrared; SWIR2) are exploited. Three conditions are used to determine the range of values that are most likely to correspond to floating vegetation for the study area. These conditions were identified using histogram analysis based on the knowledge about the spectral behavior of water and plants. Discriminating thresholds are set accordingly. Specifically, for the study area it is experimentally identified that a) the B05/B11 ratio has to be between 0.6 and 1.5, b) the Normalized Difference Water Index (NDWI) ((B08-B11)/(B08+B11)) has to be between 0.2 and 0.45, and c) the B12 band value has to be between 100 and 900.

In the third phase the results from the second phase about the presence of floating vegetation are superimposed over the previous results of the first phase and the areas found as floating vegetation replace any other underlying class. At the end a map is produced, where all three classes are evident.

Accuracy assessment was performed with the help of overall, user's accuracy (UA) and producer's accuracy (PA) metrics. The overall accuracy (OA) is calculated from the division of the number of the correctly classified pixels by the total number of the sampled pixels. The PA of each class, also called precision, is the number of the correctly classified pixels in this class divided by the number of reference pixels in this class. The PA shows the false negative predictions and compares the classified map with the producers' expectations. The UA highlights the false positives, and it is calculated from the number of the correctly predicted pixels of each class, divided by the number of the pixels that have been classified in this class and indicates how each classified pixel on the map represents the class on the ground.

3 RESULTS AND DISCUSSION

In Fig. 4 and 5 high OA for all classes is observed ranging from ~92% to 97%. The OA appears not to be influenced by the day difference between the spaceborne and ground data acquisition dates, since even when taken 25 days apart, the OA remains relatively stable (Fig. 4, 5). However, this is not a consistent remark, as lower OA appears in the year 2018 (11/08/2018), where the time interval is 20 days. This is to be accounted merely to the emergent and floating vegetation detection performance, which appears to drop further when two datasets are timely apart (see specifically the PA chart – Fig. 4).

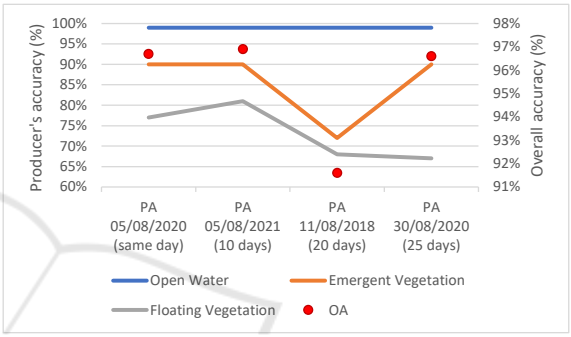

Figure 4: Producer's accuracy (in parenthesis the day difference from the acquisition date of the ground reference data).

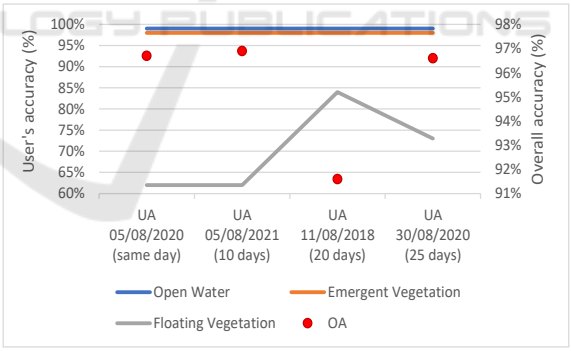

Figure 5: User's accuracy (in parenthesis the day difference from the acquisition date of the ground reference data).

Overall high OA (> 91%) at all dates is in this case misleading for the performance of the approach in each class, as the assessed dataset is imbalanced. Namely, the average reference area over all dates of the class 'Open Water' was 247.87 km^2 (71.86% of the area), followed by 89.01 km^2 (25.80% of the area), which were covered with 'Emergent Vegetation', and 8.07 km^2 (2.34% of the area) dominated by 'Floating Vegetation' (Fig. 6). Thus, the detailed analysis with the support of PA and UA is required.

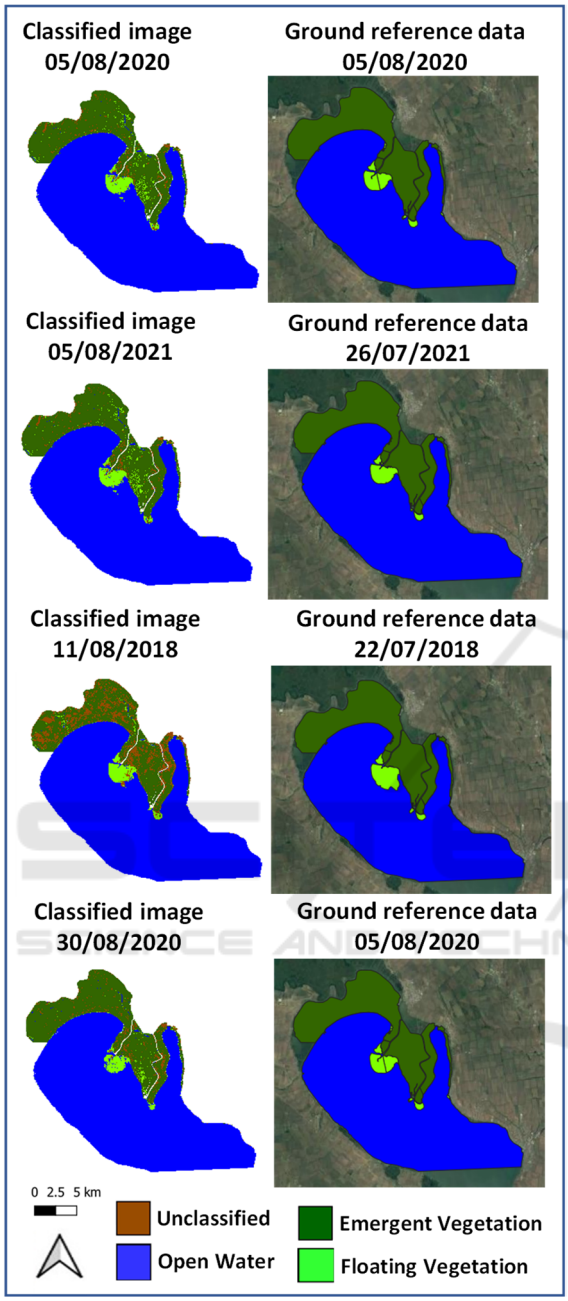

Figure 6: Aquatic vegetation maps on different dates (on the left) juxtaposed against the ground reference data (overlaid on Google Earth image snapshot) (on the right). Snapshot maps are arranged from top to bottom according to the timeliness of image vs. ground data acquisition dates.

In general, for all four validation dates, the highest PA is shown in the class of 'Open Water', followed by the class 'Emergent Vegetation' and the 'Floating Vegetation' with the lowest PA. Latter demonstrates the challenges that are posed for this class to be accurately discriminated from the surrounding environment. Furthermore, the PA is higher for the 'Floating Vegetation' class, when the reference and classification dates are timely close. This observation might be attributed to (i) the actual change of floating vegetation distribution, and/ or (ii) wind-induced floating vegetation polygon's density/ geometry change/ shift, and/ or (iii) wave- or water-level-induced floating plant leaves moistening/ partial flooding in the estuary during these intervals.

In contrary to the PA, where both emergent and floating vegetation showcase an undulated pattern through time, the UA seems not influenced for the emergent vegetation and remains stable through time, which however is not the case for the floating vegetation (Fig. 5).

In addition to the aforementioned (see PA results explanation) possible reasons for the lower performance identifying water lilies and chestnuts (floating vegetation in our study area), it is registered that this type of classification error depends also on the floating vegetation species and the density-level. In Midwood *et al.* (2010) different wetlands in the lake have been tested and the PA was higher in high-density floating vegetation and the UA was higher in low-density floating vegetation. Similar results are reached in the study of the lake Luupuvesi in Finland (Valta-Hulkkonen *et al.*, 2004), where the dense floating vegetation has higher PA, and the sparse floating vegetation has higher UA. This seems to be true for the study area and time of data acquisition, as well. In July/August (until there is no strong flooding) wind may substantially change the geometry and density of floating vegetation appearance within hours-to-days, as well as even move the water lilies and water chestnut formations (polygons). High waves (occurring in large-scale shallow water bodies) may also break the polygons, by uprooting floating rooted plant and move them.

4 CONCLUSIONS

The proposed unsupervised approach showed high overall accuracy ranging from 92% to 97% on various dates between 2018 and 2021, when classifying the study area into three classes: open water, emergent vegetation, and floating vegetation. It is found that among the four validation dates, the open water class had the highest OA, PA and UA, followed by the emergent vegetation class, while the floating vegetation class had the lowest performance (PA between 67% - 81%, and UA between 61% – 84%), indicating challenges in the discrimination and monitoring of this class from space. The PA for the

floating vegetation class improved and the UA got lower, when the reference and classification dates were timely closer. This may be accounted to (i) floating vegetation formation density/ geometry (in line with international literature findings), (ii) floating vegetation formation density/ geometry alterations due to hydrometeorological disturbance with time, and/ or (iii) changes in the distribution of floating vegetation in the estuary through time (for timely more apart reference and classification dates).

Further experimentation is required, where ground reference data allow, to enhance the transferability of the approach. Reference data acquisition across additional sites may allow testing strict thresholding performance and possibly evolving adaptive thresholding techniques; thus, leading to generalization of the approach. Ground data may also support augmenting the suggested approach by encompassing submerged aquatic vegetation mapping. This is still a challenge for Earth Observation due to the influence of the water column on the reflected signal.

ACKNOWLEDGEMENTS

This research has received funding from the European Union's Horizon 2020 Research and Innovation Action programme under Grant Agreement 101004157 – WQeMS, and was partially supported by the GEF-UNEP funded 'Towards INMS' project (www.inms.international). Ground reference data were acquired within the projects NDR#602 funded by the Ministry of Education and Science of Ukraine (2020-2022) and ENI CBC BSB PONTOS (Grant Agreement: BSB 889).

REFERENCES

Ade, Christiana, *et al.* "Genus-level mapping of invasive floating aquatic vegetation using Sentinel-2 satellite remote sensing." Remote Sensing 14.13 (2022): 3013.

Chen, Qi, *et al.* "A new method for mapping aquatic vegetation especially underwater vegetation in Lake Ulansuhai using GF-1 satellite data." Remote Sensing 10.8 (2018): 1279.

Espel, Diane, et al. "Submerged macrophyte assessment in rivers: An automatic mapping method using Pléiades imagery." Water Research 186 (2020): 116353.

Greenfield, B. K., G. S. Siemering, J. C. Andrews, M. Rajan, S. P. Andrews Jr., Spencer D. F. (2007). Mechanical shredding of water hyacinth (Eichhornia crassipes): Effects on water quality in the Sacramento-San Joaquin River Delta, California. Estuaries and Coasts, 30, 627-640.

Kordelas, Georgios A., *et al.* "Fast and automatic data-driven thresholding for inundation mapping with Sentinel-2 data." Remote Sensing 10.6 (2018): 910.

Kovalova, N., Medinets, V., Medinets, S. (2021). Peculiarities of Long-Term Changes in Bacterioplankton Numbers in the Dniester Liman. Hydrobiological Journal, 57, 27-36.

Manakos, I., Kordelas, G., Marini, K. (2019). Fusion of Sentinel-1 data with Sentinel-2 products to overcome non-favourable atmospheric conditions for the delineation of inundation maps. European Journal of Remote Sensing, DOI: 10.1080/22797254.2019.1596757.

Medinets, S. (2014). The Black Sea nitrogen budget revision in accordance with recent atmospheric deposition study. Turkish Journal of Fisheries and Aquatic Sciences, 14, 981-992.

Medinets, S. and Medinets, V. (2012). Investigations of atmospheric wet and dry nutrient deposition to marine surface in western part of the Black Sea. Turkish Journal of Fisheries and Aquatic Sciences, 12, 497-505.

Medinets, S., Gasche, R., Skiba, U., Medinets, V., Butterbach-Bahl, K. (2016). The impact of management and climate on soil nitric oxide fluxes from arable land in the Southern Ukraine. Atmospheric Environment, 137, 113-126.

Medinets, S., Kovalova, N., Medinets, V. *et al.* (2020a). Assessment of riverine loads of nitrogen and phosphorus to the Dniester Estuary and the Black Sea over 2010-2019. In Monitoring of Geological Processes and Ecological Condition of the Environment. EAGE. https://doi.org/10.3997/2214-4609.202056029

Medinets, S., Mileva, A., Kotogura, S. *et al.* (2020b). Rates of atmospheric nitrogen deposition to agricultural and natural lands within the Lower Dniester catchment. In Monitoring of Geological Processes and Ecological Condition of the Environment. EAGE. https://doi.org/10.3997/2214-4609.202056053

Midwood, Jonathan D., and Patricia Chow-Fraser. "Mapping floating and emergent aquatic vegetation in coastal wetlands of Eastern Georgian Bay, Lake Huron, Canada." Wetlands 30 (2010): 1141-1152.

OSCE (2005). Transboundary diagnostic study for the Dniester river basin. Project Report, November 2005. OSCE/UNECE publication, 94 p.

Rouholahnejad, E., Abbaspour, K. C., Srinivasan, R., Bacu, V., Lehmann, A. (2014). Water resources of the Black Sea Basin at high spatial and temporal resolution. Water Resources Research, 50, 5866-5885.

Sutton, M.A., Howard, C.H., Erisman, J.W. *et al.* (2011). The European nitrogen assessment. Cambridge: Cambridge University Press.

Valta-Hulkkonen, Kirsi, A. Kanninen, and P. Pellikka. "Remote sensing and GIS for detecting changes in the aquatic vegetation of a rehabilitated lake." International Journal of Remote Sensing 25.24 (2004): 5745-5758.